

Silicone-Rubber Indentation Simulation using Meshfree Method Based on Radial Basis Function

Juan F. Ramírez-Salazar^{a*}, Elizabeth Mesa-Múnera^a, Pierre Boulanger^b and John W. Branch^a

^aDepartment of Systems Engineering., National University of Colombia, Medellín, Colombia;

^bDepartment of Computing Science, University of Alberta, Edmonton, Canada.

ABSTRACT

This paper presents a meshfree method to simulate the interaction between a rigid body and soft tissue. A simple orthogonal indentation on a prototype model with similar properties than biological soft tissue was simulated using Radial Point Interpolation Meshfree Method. The results were validated with an experiment, where the penetration forces and deformations were measured with high resolution position, force, and torque sensors. The measured results were then compared to a meshfree method simulation predictions from the point of view of force and global deformation accuracy. The results show the potential of the Meshfree method in predicting biological soft tissue deformations during tool-tissue interaction in surgical simulators.

Keywords: Radial Point Interpolation, Meshfree Methods, Orthogonal Indentation

1 INTRODUCTION

Needle insertion is a common procedure performed in surgical environments with variable complexity. They include procedures as simple as subcutaneous vaccination and as complex as needle insertion within the brain to extract a tumoral sample. Many of those procedures are performed by the surgeon relying on the kinesthetic feedback through the tool, and correlated with their own mental model of human anatomic structures. In most of the cases, surgical procedure of this nature requires meticulous execution in order to reduce post-operating complications and improve overall patient outcome.

In recent years, the use of training system based on virtual reality has been increased significantly. These systems introduce an ideal alternative for the evaluation and training of health care practitioner. As a result, the paradigm of surgical training has moved from inanimate models, corpse, and animals, to include complex virtual training system systems that incorporate video displays and haptic devices. Virtual Reality based training systems for catheter insertion, epidural lumbar puncture, spine biopsy, breast biopsy, neurosurgical probe insertion, prostate needle biopsy, among others, constitute part of today's trend toward computer based simulators for medical and surgical training [1]. Even experienced surgeons benefit from this type of systems to plan and test highly complex procedures, and to design or test new surgical tools [2].

Behind every surgical system there are mathematical models that predict the mechanical behaviour of biological tissues. Different methods have been used to perform those simulations. Finite Element Methods (FEM) is one technique that has been widely used and accepted in the medical simulation community. However, it is not without shortcomings, among the most outstanding shortcoming of FEM is that it relies on meshes or elements that are connected together by nodes in a properly defined manner. For that reason, considerable accuracy is lost when handling large deformation because of the element distortion [3] as in the case of human organs, which undergoes large deformations under relatively low stress [4].

Most existing simulations for needle insertion are based on FEM, for which the special domain of both the tissue and the needle is discretized into a mesh of elements. Those approaches usually require re-meshing or mesh modification due to the element distortion. Re-meshing procedures is usually theoretically complicated and computational expensive, especially for high order elements. Numerous simulations of needle insertion using mesh-based method are reported in the literature. Abolhassani et. al present in [5] an extensive survey of needle insertion simulation into soft tissue. They conclude that among several challenges, there is a necessity to improve the current numerical models to integrate other complex scenarios with different biomechanical models.

*Corresponding author. E-mail: jframiresa@unal.edu.co.

Needle insertion forces have been studied for gelatin [6], ex-vivo porcine tissue [7] [8], bovine samples [9]. In each case, the resultant force acting at the needle end was measured. DiMaio et.al [10] presented a planar virtual environment for needle insertion, which was developed based on a static linear finite element model and estimated the needle shaft forces and tissue behavior. In [11], they implement a meshfree method using Moving Least Square approximation to analyze the deflection of a bevel-tip flexible needle. They demonstrate that different from mesh-based approaches, meshfree approach allows higher numerical accuracy.

This paper presents some preliminary results of our work, whose ultimate goal is to simulate needle insertion into biological soft tissue using meshfree methods. We evaluate the performance of the Radial Point Interpolation Meshfree Method (RPIM), to simulate a mechanical indentation on a silicone-rubber material with similar properties to biological soft tissues. A 2D implementation of the method and an indentation experiment using position, force and torque sensor was carried out to validate the simulation results.

2 METHODS AND MATERIALS

In meshfree methods, instead of discretizing the special domain into elements, as in FEM, the domain is represented by a set of nodes bounded by the boundary domain. The density of the nodes depends on the accuracy expected to reach. Due to the low speed of the indenter, this problem was analyzed as static. The partial differential equation and boundary conditions for the simulation are:

$$\text{Equilibrium Equation:} \quad \mathbf{L}^T \boldsymbol{\sigma} + \mathbf{b} = \mathbf{0}, \text{ in } \Omega, \quad (1)$$

$$\text{Natural boundary condition:} \quad \boldsymbol{\sigma} \mathbf{n} = \mathbf{t}, \text{ in } \Gamma_i, \quad (2)$$

$$\text{Essential boundary condition:} \quad \mathbf{u} = \bar{\mathbf{u}}, \text{ in } \Gamma_u, \quad (3)$$

where, \mathbf{L} is the differential operator, $\boldsymbol{\sigma}$ is the stress tensor, \mathbf{u} is the displacement vector, \mathbf{b} is the body force vector, \mathbf{t} is the prescribed traction vector, $\bar{\mathbf{u}}$ is the prescribed displacement vector, and \mathbf{n} is the outward normal vector. The last three variables are considered on the boundary domain (Γ).

The standard variational (weak) form of the system equations from (1) to (3) is posed as Equation (4) [3], where \mathbf{D} is the matrix of elastic constants and Ω is the problem domain, see [12] for more detail.

$$\int_{\Omega} (\mathbf{L}\delta\mathbf{u})^T (\mathbf{D}\mathbf{L}\mathbf{u}) d\Omega - \int_{\Omega} \delta\mathbf{u}^T \mathbf{b} d\Omega - \int_{\Gamma} \delta\mathbf{u}^T \bar{\mathbf{t}} d\Gamma = 0. \quad (4)$$

From the previous equation, the interest is to find the deformed state of the domain, which is described by the vector \mathbf{u} (displacement). We select a radial basis function (RBF) approximation as it has been proven to be more robust at simulating mechanical deformation and allows to create shape functions that possesses the delta function property. The approximation function for Equation (4) is defined by Equation (5) which uses a multiquadratics radial basis function, Equation (6),

$$\mathbf{u}^h(x) = \sum_{i=1}^n R_i(x) a_i(x_Q) = \mathbf{R}^T(x) \mathbf{a}(x_Q), \quad (5)$$

$$R_i(x, y) = (r_i^2 + (a_c d_c)^2)^q, \quad a_c \geq 0, \quad (6)$$

where a_c and q are dimensionless shape parameters. The variable n is the number of nodes into the quadrature support domain and r_i is the distance between each couple nodes. The parameter d_c is a characteristic length that relates to the nodal spacing in the local support domain of the point of interest \mathbf{x} , and it is usually the average nodal spacing for all the nodes in the local support domain. The simplest method to define d_c is:

$$d_c = \frac{\sqrt{A_s}}{\sqrt{n_{A_s}} - 1}, \quad (7)$$

where A_s is an estimated value of the area of the local support domain, and n_{A_s} is the number of nodes cover by the local support domain.

In order to perform a tractable numerical simulation, an axisymmetric model was constructed. Only half of the domain of interest was discretized due to the symmetry of the phenomenon. The discretized model was design to provide a high-density of nodes at the contact region. A total of 691 irregular distributed nodes were created as plotted in Figure 2(a). A total of 231 (11×21) regularly rectangular background cells were used for numerical integration. The other parameters of the RBF were set up as: $a_c = 2$, $q = 1.03$. The boundary conditions are set to be: $u_y = 0$ and $u_x = 0$ along the nodes for $y = 0$. Along the left contour (mirror axis, $x = 0$), we defined $u_x = 0$. Furthermore, the nodes on the contact region were set as: $u_y = -10\text{mm}$ and $u_x = 0$, assuming static friction between the indenter and the model.

2.1 Experiment

In the validation process, we used a silicon model of $70 \times 80 \times 80 \text{ mm}$ made of 2-part Silicone Rubber (Ecoflex 00-10, from Smooth-On) which as demonstrate to be similar to soft tissue properties [13]. The material is soft but exhibits linear behavior for small deformation. A small strain uniaxial compression test was performed on the model to obtain the elastic material properties, see Figure 1(a). Results indicate a Young's modulus of (6.96 *KPa*), and a Poisson's ratio of 0.4999 (assuming incompressible continua material) was used.

The cube was submitted to an orthogonal indentation with an indenter of 10 *mm* in diameter attached to a force/torque sensor, (ATI Mini40 SI-40-2) with 0.02 *N* resolution. The indenter was displaced at a constant velocity of 0.4 *mm/s* until the model was deformed by 10 *mm*. The deformed surface was scanned using a high precision 3D laser scanner from Kreon mounted on a FARO arm as shown in Figure 1(b).

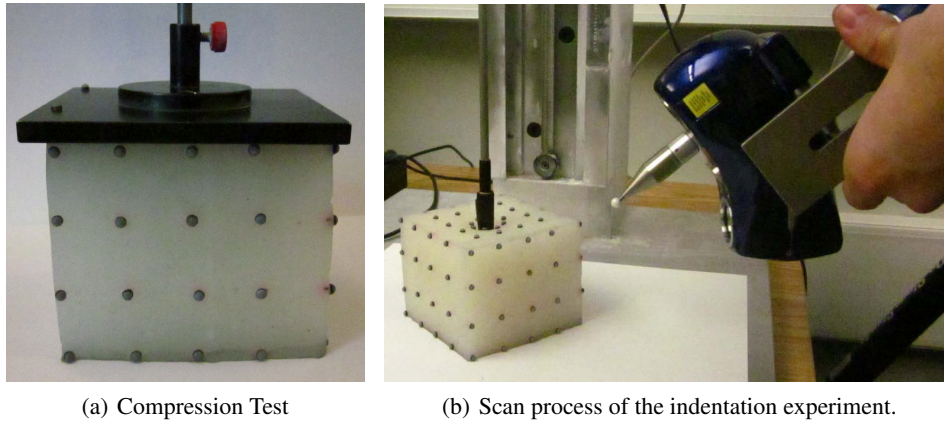


Figure 1. Experimental setups.

3 RESULTS

We simulate the vertical indentation assuming homogeneous and isotropic material. Figure 2 presents the discretized domain and the simulated results. The 3D scanned model for the indentation experiment is presented in Figure 3.

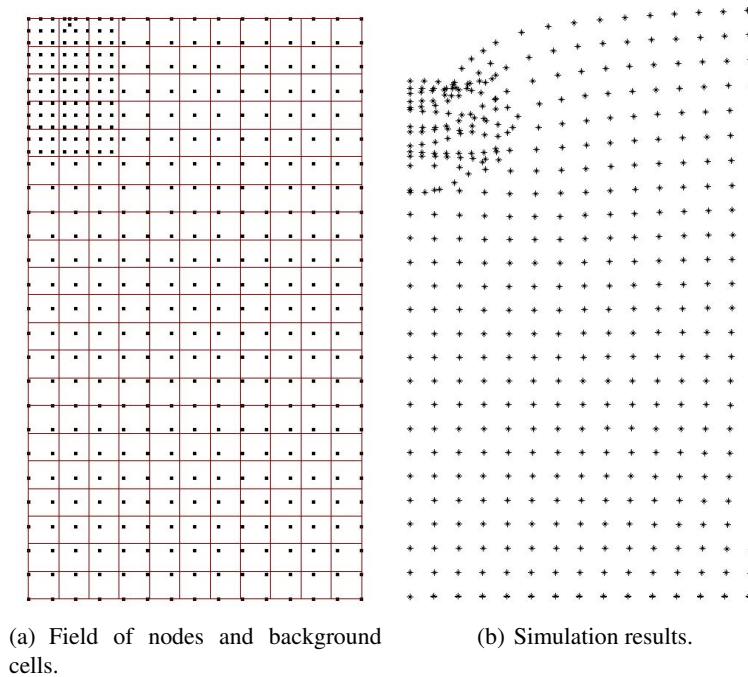


Figure 2. Un-deformed and deformed stage.

In order to compare the simulation and the experiment results, it was necessary to extract the contour line for the middle plane of the scanned model. Besides, we create a mirror of the outline from the simulation to validate

the symmetry of the experiment. Both curves were register using the nodes placed in the bottom plane, because we ensured zero displacement for them. The 3D reconstruction process of the scanned model, as well as the registration was carried out using the software Rapidform V2006.

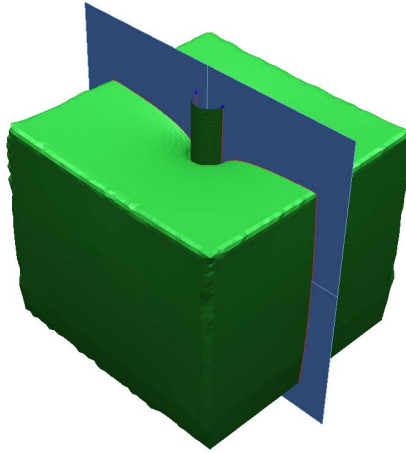


Figure 3. 3D model reconstructed from the indentation experiment.

The maximum force measured with the force sensor was 2.71 N and the simulated value was 2.45 N , which correspond to error of 11% of relative error. As for the deformation variable, the highest difference between both curves was located in the surrounding area of the indenter with 1.71 mm of deviation, as shown in Figure 4.

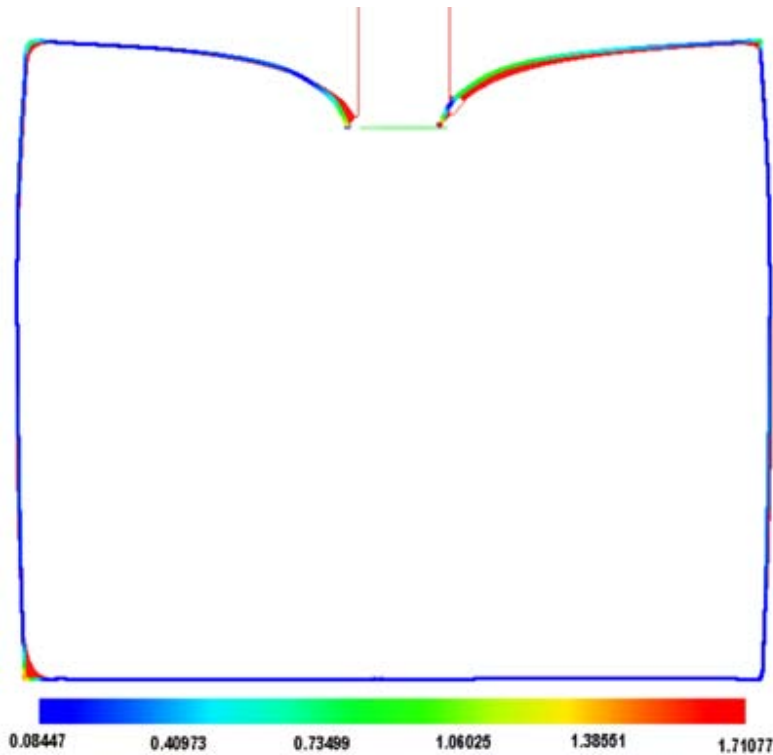


Figure 4. Comparison of the outline curve from the simulation and the scanned model (units in millimeters).

4 CONCLUSION

In this work, we present a meshless method to simulate indentation on biological soft tissue, in a different way from the classic mesh-based approaches. We demonstrate that RPIM is a straightforward alternative to simulate large tissue deformation using FEM. Furthermore, this method has high potential to be extended to actual needle insertion

within the tissue. Based on our results we consider our simulation to be accurate in magnitude, but only on the linear elastic behavior. The higher deformation values are attained near to the indentation area, where the highest value is around 1.71 *mm* of deviation. As future work, we are planning to implement the same method to simulate 3D models with complex geometries and different mathematical formulation, and we will implement the visibility criterion [14] method to simulate a real insertion within the tissue.

References

- [1] D. Cooke, R. Jamshidi, J. Guitron, and J. Karamichalis, "The virtual surgeon: Using medical simulation to train the modern surgical resident," *BULLETIN-AMERICAN COLLEGE OF SURGEONS* **93**(7), p. 26, 2008.
- [2] A. Trejo, M. Jung, D. Oleynikov, and M. Hallbeck, "Effect of handle design and target location on insertion and aim with a laparoscopic surgical tool," *Applied Ergonomics* **38**(6), pp. 745–753, 2007.
- [3] G. Liu, *Meshfree methods: moving beyond the finite element method*, CRC, 2009.
- [4] Y. Fung, *Biomechanics: mechanical properties of living tissues*, Springer, 1993.
- [5] N. Abolhassani, R. Patel, and M. Moallem, "Needle insertion into soft tissue: A survey," *Medical engineering & physics* **29**(4), pp. 413–431, 2007.
- [6] L. Hiemenz, A. Litsky, and P. Schmalbrock, "Puncture mechanics for the insertion of an epidural needle," in *Proceedings of the Twenty-First Annual Meeting of the American Society of Biomechanics*, 1997.
- [7] P. Brett, T. Parker, A. Harrison, T. Thomas, and A. Carr, "Simulation of resistance forces acting on surgical needles," *Proceedings of the Institution of Mechanical Engineers, Part H: Journal of Engineering in Medicine* **211**(4), pp. 335–347, 1997.
- [8] C. Simone and A. Okamura, "Modeling of needle insertion forces for robot-assisted percutaneous therapy," in *Robotics and Automation, 2002. Proceedings. ICRA'02. IEEE International Conference on*, **2**, pp. 2085–2091, IEEE, 2002.
- [9] A. Okamura, C. Simone, and M. O'Leary, "Force modeling for needle insertion into soft tissue," *Biomedical Engineering, IEEE Transactions on* **51**(10), pp. 1707–1716, 2004.
- [10] S. DiMaio and S. Salcudean, "Needle insertion modeling and simulation," *Robotics and Automation, IEEE Transactions on* **19**(5), pp. 864–875, 2003.
- [11] J. Xu, L. Wang, K. Wong, and P. Shi, "A meshless framework for bevel-tip flexible needle insertion through soft tissue," in *Biomedical Robotics and Biomechatronics (BioRob), 2010 3rd IEEE RAS and EMBS International Conference on*, pp. 753–758, IEEE.
- [12] G. Liu and S. Quek, *The finite element method: a practical course*, Butterworth-Heinemann, 2003.
- [13] H. Mansy, J. Grahe, and R. Sandler, "Elastic properties of synthetic materials for soft tissue modeling," *Physics in Medicine and Biology* **53**, p. 2115, 2008.
- [14] X. Zhuang, C. Augarde, and S. Bordas, "Accurate fracture modelling using meshless methods, the visibility criterion and level sets: Formulation and 2d modelling," *International Journal for Numerical Methods in Engineering* **86**(2), pp. 249–268, 2011.